Journal of
Mechanics of
Materials and Structures

DEPLOYMENT PROCEDURE FOR THE TETRAHEDRON CONSTELLATION

Pedro A. Capó-Lugo and Peter M. Bainum

Volume 4, Nº 5 May 2009

mathematical sciences publishers

JOURNAL OF MECHANICS OF MATERIALS AND STRUCTURES
Vol. 4, No. 5, 2009

DEPLOYMENT PROCEDURE FOR THE TETRAHEDRON CONSTELLATION

PEDRO A. CAPÓ-LUGO AND PETER M. BAINUM

The NASA Benchmark Tetrahedron Constellation is a four-satellite formation that requires a nominal separation distance at every apogee point. The deployment procedure of a tetrahedron constellation is complex and depends on the separation distance between any pair of satellites within the constellation. In this paper, the deployment procedure of the tetrahedron constellation will be divided into two stages: the deployment from a circular parking orbit to an elliptical orbit, and the correction of the separation distance between pairs of satellites within the constellation. The solution of this problem will be implemented with a combination of Hohmann transfer maneuvers and the digital linear quadratic regulator control scheme showing a minimum consumption of fuel. In summary, the combination of these two techniques will provide a different approach to the deployment procedure of the NASA benchmark tetrahedron constellation.

1. Introduction

One concern in the NASA Benchmark Tetrahedron Constellation problem [Carpenter et al. 2003] is the deployment and reconfiguration procedures. Some papers solved these procedures using different numerical schemes based on pseudospectral methods [Williams and Trivailo 2006; Huntington et al. 2006; Huntington and Rao 2006]. The pseudospectral method solves an optimal control problem by dividing the highly elliptical orbit into sections. In these sections, a two-point boundary value problem will be solved for coasting and thruster burning phases. To solve the pseudospectral method, the problem is transformed into another domain that contains the desired solution of the optimal control problem. After every two-point boundary value problem is solved in every section of the highly elliptical orbit, the control effort and the time for the different coasting and burning phases are mapped into the actual problem to show the solution. This numerical method may take a longer period of time to solve the optimal control problem. In addition, the pseudospectral methods involve a complex mathematical development to include different characteristics of the tetrahedron constellation. For these reasons, the objective of this paper is to present a different solution to the deployment procedure of the NASA Benchmark Tetrahedron Constellation without the use of complex mathematical models.

The satellites will be transferred from a circular orbit to an elliptical orbit with a Hohmann transfer maneuver [Wertz and Larson 1999]. This transfer maneuver represents the most fuel efficient procedure to obtain the desired elliptical orbit for the four satellites. The Hohmann transfer orbit has been used to deploy a different tetrahedron constellation as shown in [Dow et al. 2004]. Also, Bainum et al. [2005] have showed that, by using a modified Hohmann transfer, an along-track constellation can be launched

Keywords: discrete linear quadratic regulator, impulse maneuvers, deployment procedure, tetrahedron constellation.
Research supported by Alliances for Graduate Education and Professoriate (AGEP) Program.

from a circular orbit to an elliptical orbit. With these maneuvers, the satellites in the along-track constellation reach the required configuration at the final apogee point. A similar procedure can be used here to achieve the final formation for the proposed tetrahedron constellation.

After the Hohmann transfer maneuver is used, the digital linear quadratic regulator (DLQR) will be used to correct the drifts in the separation distance and the velocities between any pair of satellites within the constellation. This DLQR control scheme can be used to provide a faster solution to the correction of the separation distances and velocities between any pair of satellites within the proposed constellation. A thrust requirement will be included into the formulation of the DLQR active control scheme to determine the consumption of force during the drift correction.

The purpose of this research work is to present a combination of two techniques to finally deploy the NASA Benchmark Tetrahedron Constellation from an along-track circular orbit to a highly elliptical orbit. With this scheme, a different solution will be provided to obtain the deployment procedure without the use of complex mathematical models and methods.

2. Desired conditions of the satellites in the proposed tetrahedron constellation

The tetrahedron constellation will be used to measure the components of the Earth's magnetic field with the critical data taken at the apogee point by magnetometers. In order to obtain a precise mapping of the Earth's magnetic field, it is important that the positions of all the instruments be accurately placed at or near the apogee point.

According to the NASA Benchmark problem [Carpenter et al. 2003] definition for the tetrahedron constellations, the nominal separation distance between any two of the satellites at apogee is 10 km, and the separation error at subsequent apogees should be within 10%, giving an acceptable range between 9 and 11 km. At other points in the orbit, the minimum separation distance between any pair of satellites should be 1 km. Figure 1 shows a representation of the tetrahedron constellation at the apogee point. SB and SC are assumed to be located along the semimajor axis with a separation distance of 10 km. SA forms the equilateral triangle and is orbiting around the centroid in the equilateral triangle. SH is the fourth satellite located above the centroid of the equilateral triangle which forms the tetrahedron constellation.

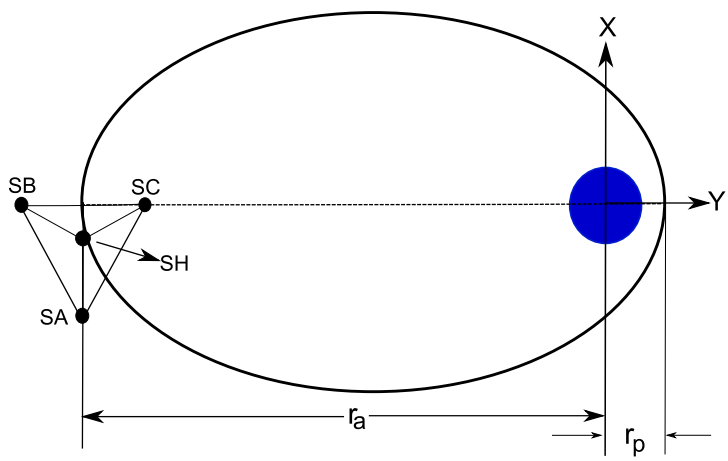

Figure 1. Two dimensional view of the configuration at apogee point.

	SA	SB	SC	SH
X (km)	−8.6602	0	0	−2.8868
Y (km)	−72582.4525	−72587.1941	−72577.7109	−72585.0433
Z (km)	−24285.7489	−24287.3354	−24284.1624	−24278.0058
V_x (km/sec)	0.973083288	0.972733623	0.973432881	0.973083324
V_y, V_z (km/sec)	0	0	0	0

Table 1. Satellite initial positions and velocities for Phase I.

	SA	SB	SC	SH
a (km)	42095.7	42095.7	42095.7	42095.7
e	0.818182	0.818301	0.818064	0.818182
i (degrees)	18.5	18.5	18.5	18.494
Ω (degrees)	0	0	0	0
ω (degrees)	89.9921	90	90	89.9974

Table 2. Orbital elements for the four satellites within the constellation (Phase I).

Using the techniques explained in [Capó-Lugo and Bainum 2005; 2006b], the constellation has a similar configuration at the perigee point, and the tetrahedral formation is obtained with the required separation distance constraints at the apogee point. These techniques were based on the orbital elements of the constellation and did not contain an active control scheme to satisfy the separation distance conditions of the NASA Benchmark Tetrahedron Constellation.

For the first specific size (phase I) of the proposed constellation [Carpenter et al. 2003], the initial positions and velocities for the four satellites are expressed in Table 1. These initial coordinates and velocities are the required conditions such that the final tetrahedron constellation can be obtained at the apogee point. Without perturbations [Capó-Lugo and Bainum 2005; 2006b], the satellites in the constellation satisfied the separation distance constraints for a long period of time, and, with perturbation, the constellation maintains the separation distance conditions for a limited number of complete orbits. For phase I, Table 1 can be used to define the orbital elements for every satellite. Table 2 shows the desired orbital elements at the final apogee point which will be used to calculate the Hohmann transfer maneuvers. In Table 2, a is the semimajor axis, e is the eccentricity, i is the inclination angle, Ω is the right ascension of the ascending node, and ω is the argument of perigee.

3. Transfer from a circular orbit to the elliptical orbit (Stage 1)

The transfer procedure from a circular orbit to an elliptical orbit is complex and may take a period of time before it is achieved. Dow et al. [2004] used a modified Hohmann transfer maneuver to transfer four satellites from a circular orbit to a final elliptical orbit. In their paper, a small consumption of fuel was obtained because the tetrahedron constellation was deployed using intermediate elliptical orbits. If the satellites are in a circular orbit and are transferred to an elliptical orbit with an eccentricity of 0.8, as

an example, the intermediate elliptical orbit is defined as the chosen intermediate values of eccentricity (between 0 and 0.8) used to perform the Hohmann transfer maneuvers.

On the contrary, [Bainum et al. 2005] show that a modified Hohmann transfer orbit can be used to deploy an along-track constellation from a circular parking orbit to an elliptical orbit. In this technique, the satellites are deployed with restrictions on the period of the transfer orbit; in this way, the satellites can reach the apogee point at the same time in the along-track constellation. The required difference in velocity (ΔV) [Bainum et al. 2005] to transfer the satellites from the circular to the elliptical transfer orbit is very similar for all of them which are a characteristic of the modified Hohmann transfer maneuvers.

This section will use similar modified Hohmann transfer maneuvers [Bainum et al. 2005] to transfer the four satellites from a circular orbit into their respective elliptical orbits. After the satellites are released from a rocket, the four satellites will be assumed to be in a circular orbit forming an along-track configuration; also, the separation distance between any pair of satellite within the constellation will be assumed constant. It will be also assumed that the circular orbit will have an inclination angle of 18.5° and a radius equal to 1.2ER, where ER means Earth radius. As shown in [Capó-Lugo and Bainum 2005; 2006b], this is the radius of perigee and inclination angle for phase I. Before the difference in velocity for the Hohmann transfer maneuvers is calculated, the period of the transfer orbit for every satellite must be studied to determine the order in which the satellites will be deployed. The period of a satellite is defined as

$$T = 2\pi\sqrt{\frac{a^3}{\mu}}. \tag{1}$$

To calculate the semimajor axis (a), the radius of perigee (r_p) for every satellite is set equal to 1.2ER, and the radius of apogee will be defined for every satellite depending on the desired eccentricity and semimajor axis as shown in Table 2. Table 3 illustrates the radius of apogee (r_a), semimajor axis for the transfer orbit (a_t), and the transfer period for every satellite (T_t).

It can be seen from Table 3 that SB and SC, respectively, has the highest and smallest period in comparison with the satellites SA and SH. The period of the four satellites provides the order in which the satellites will be departing from the circular orbit. The first satellite to depart is SB because it has the highest period. The second satellite is SA because it must be ahead of SH to form the equilateral triangle. The third satellite to depart from the circular orbit will be SH. This satellite will be in the same plane as the other three satellites, but, after the transfer maneuvers, it will be corrected with the DLQR to exhibit out-of-plane motion. The last satellite to depart in the circular orbit is SC which has the smallest period. The separation distance between the satellites in the circular orbit will be considered because, at the final apogee point, it will make a difference in the separation distance between any pair of satellites within the constellation in the final elliptical orbit.

The deployment procedure from the circular orbit to the elliptical orbit is defined as follows:

	SA	SB	SC	SH
r_a (km)	76537.64	76545.388	76532.638	76537.64
a_t (km)	42095.70	42099.58	42093.20	42095.70
T_t (sec)	85910.72	85922.59	85903.07	85910.72

Table 3. Radius of apogee, semimajor axis of the transfer orbit, and period for every satellite.

1. After the four satellites are released from the rocket, these satellites are assumed to be traveling in a circular orbit forming an along-track constellation. The circular orbit has a radius equal to 1.2ER, and it is assumed that the orbit has an inclination angle equal to 18.5°. Initially, the satellites are assumed to be separated by 0.5° in the true anomaly angle. This difference in the true anomaly angle between any pair of satellites can be changed to larger values, but, at the final apogee point of the transfer ellipse, the separation distance between any pair of satellites will be higher. In addition, the satellites may not reach the apogee point at the same time; for this reason, the separation in the true anomaly angle between some of the pairs of satellites in the along track constellation will be constrained to angles between 0 and 1 degree. Figure 2 shows the difference in the true anomaly angle between the satellites in the along-track constellation in the circular orbit. In Figure 2, δf is the difference in the true anomaly angle, f is the true anomaly angle, and the center of the Earth is denoted by the center of the Cartesian system X and Y. The difference in the true anomaly angle is assumed equal to 0.5° and creates a separation distance of approximately 66.79 km between the pairs SB-SA, SA-SH, and SH-SC in the along-track constellation. The four satellites have a velocity in the circular orbit equal to 7.2166 km/sec. As said earlier, the first satellite to be deployed is SB. The semimajor axis of the transfer orbit for SB is defined in Table 3, and the velocity at the perigee point in the elliptical transfer orbit is equal to

$$V_{p,\mathrm{SB}} = \sqrt{\mu\left(\frac{2}{r_p} - \frac{1}{a_t}\right)} = 9.73088\,(\mathrm{km/sec}). \tag{2a}$$

The necessary ΔV to transfer SB from the circular orbit to the elliptical transfer orbit is equal to

$$\Delta V_{P,\mathrm{SB}} = 9.73088 - 7.2166 = 2.5148\,(\mathrm{km/sec}). \tag{2b}$$

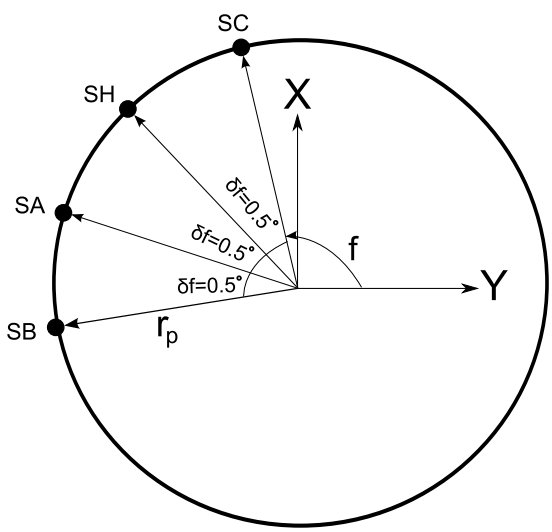

Figure 2. Location and separation of the four satellites in the circular orbit.

This ΔV maneuver is applied in the direction of the motion of the satellite to increase its velocity such that the satellite can be transferred into the elliptical orbit. This ΔV procedure will be performed when the true anomaly angle is equal to 90° because, when the satellite is in the elliptical transfer orbit, the angle at which the satellite departs will be its argument of perigee (ω).

2. 9.25 seconds after SB has departed, SA will be at the transfer point in the circular orbit ($f = 90°$). From Table 3, the difference in the period of the transfer orbit between SB and SA is 11.87 seconds. A correction to the period of the transfer orbit is not necessary because SA will be 2.62 seconds ahead of SB. This difference in time will cause SA to reach the position of SB in a short period of time. For this reason, a correction in the period of the elliptical transfer orbit for SA is not necessary. The velocity and ΔV to change SA from a circular orbit to the elliptical transfer orbit is

$$V_{p,\mathrm{SA}} = \sqrt{\mu\left(\frac{2}{r_p} - \frac{1}{a_{t,\mathrm{SA}}}\right)} = 9.7308\,\mathrm{km/sec}, \quad \Delta V_{p,\mathrm{SA}} = 9.73083 - 7.2166 = 2.5142\,\mathrm{km/sec}. \tag{3}$$

3. 9.25 seconds after SA has departed, SH has reached the transfer point in the circular orbit. The difference in the transfer period between SA and SH is zero (Table 3), but the time that SH takes to reach the transfer point provides the required condition to avoid a collision between these two satellites. For this reason, the transfer period for SH is not altered. The velocity and ΔV to maneuver SH into the elliptical transfer orbit are

$$V_{p,\mathrm{SH}} = \sqrt{\mu\left(\frac{2}{r_p} - \frac{1}{a_{t,\mathrm{SH}}}\right)} = 9.7307\,\mathrm{km/sec}, \quad \Delta V_{p,\mathrm{SH}} = 9.7307 - 7.2166 = 2.5141\,\mathrm{km/sec}. \tag{4}$$

4. 9.25 seconds after SH has departed, SC will reach the transfer point ($f = 90°$). The difference in the transfer period between SB and SC is 19.52 seconds. Once more, a correction to the period of the elliptical transfer orbit is not necessary because the time that SC takes to reach the transfer point will provide enough distance between the other three satellites to avoid a collision. The velocity and the ΔV at the transfer point required to maneuver SC into the elliptical transfer orbit can be defined as

$$V_{p,\mathrm{SC}} = \sqrt{\mu\left(\frac{2}{r_p} - \frac{1}{a_{t,\mathrm{SC}}}\right)} = 9.7308\,\mathrm{km/sec}, \quad \Delta V_{p,\mathrm{SC}} = 9.7308 - 7.2166 = 2.5142\,\mathrm{km/sec}. \tag{5}$$

5. Once the satellites have reached the apogee point, a second ΔV maneuver will be performed to correct the semimajor axis and the eccentricity of the final elliptical orbit. To perform this maneuver, the velocity of the satellite at the apogee point in the elliptical transfer orbit is calculated and, then, is subtracted from the velocity at the apogee point defined in Table 1. Table 4 shows the velocity and ΔV required for the four satellites in the constellation at the apogee point.

	SB	SA	SH	SC
V_a (km/sec)	0.97299	0.9730833	0.973083	0.97343288
ΔV_a (km/sec)	-0.2888×10^{-3}	0	0	0.2828×10^{-3}

Table 4. Velocity at the apogee point in the transfer orbit and the ΔV required to correct the in-plane conditions of the final orbit.

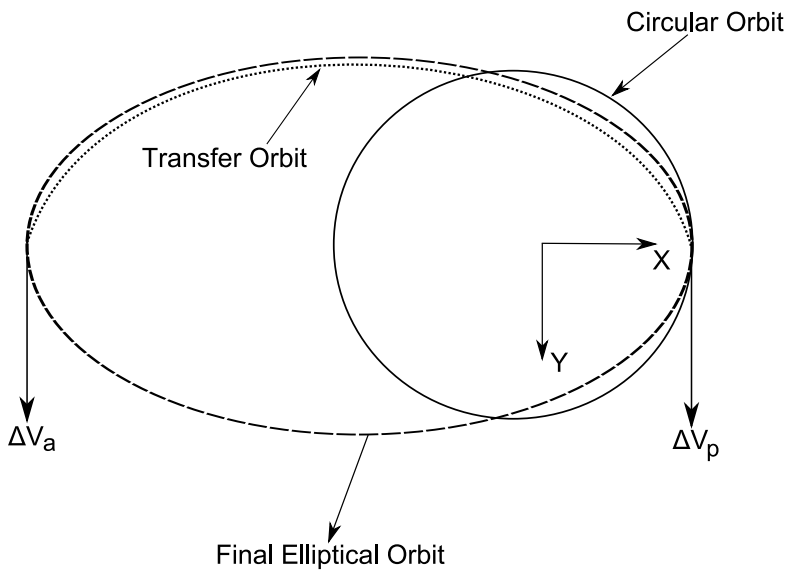

Figure 3. Diagram of the deployment procedure of the constellation.

At the apogee point, this ΔV maneuver will be also applied along the positive or negative tangential direction of the satellite. Figure 3 shows the ΔV maneuvers and the different orbits that will be obtained with these modified Hohmann transfer maneuvers. The Cartesian axis at the center of the Earth is rotated because the elliptical orbit will be created over the X axis in which the true anomaly angle is equal to 90°. This angle will define the argument of perigee of the orbit of the four satellites.

These five steps will define the elliptical orbit of the four satellites using Hohmann transfer maneuvers. Observing the transfer period of the four satellites, these satellites will reach the apogee point at the same time. The tetrahedron formation will not be obtained at the final apogee point; for this reason, a final correction of the separation distance between the satellites is required. This correction can be performed in two ways: solving a two-point boundary value problem (TPBVP) with the linearized Tschauner–Hempel equations, or correcting the drifts in the separation distance between any pair of satellites within the constellation with the DLQR controller [Capó-Lugo and Bainum 2006a].

The solution of a TPBVP is complicated because it involves the theory of primer vector defined in [Lawden 1963]. The linearized Tschauner–Hempel (TH) equations defined by Carter and Humi [1987] satisfy the primer vector relations, and the solution depends on the type of thrust arc. The solution of the TPBVP can be preferred for the formation of the tetrahedron constellation at the apogee point, but there are some other considerations related to the solution of this problem. For these reasons, the correction of the separation distance constraints for the proposed tetrahedron constellation [Carpenter et al. 2003] will be based on the DLQR control scheme [Capó-Lugo and Bainum 2006a]. With this DLQR control scheme, the tetrahedron constellation can be formed with the required separation distance at the following apogee point.

4. Linearized Tschauner–Hempel (TH) equations and thrust capability

The linearized TH equations that define the motion of a pair of satellites in an elliptical orbit about the Earth [Carter and Humi 1987] can be written as

$$y'(f) = [A(f)]\,y(f) + [B(f)]\,\vec{a}, \tag{6a}$$

where

$$[A(f)] = \begin{bmatrix} 0 & 0 & 0 & 1 & 0 & 0 \\ 0 & 0 & 0 & 0 & 1 & 0 \\ 0 & 0 & 0 & 0 & 0 & 1 \\ 0 & 0 & 0 & 0 & 2 & 0 \\ 0 & 3\kappa & 0 & 2 & 0 & 0 \\ 0 & 0 & -1 & 0 & 0 & 0 \end{bmatrix}, \qquad [B(f)] = \begin{bmatrix} 0 & 0 & 0 \\ 0 & 0 & 0 \\ 0 & 0 & 0 \\ \kappa^3 & 0 & 0 \\ 0 & \kappa^3 & 0 \\ 0 & 0 & \kappa^3 \end{bmatrix}, \tag{6b}$$

$$y_j = (1 + e\cos f)x_j, \quad y_j' = (1 + e\cos f)x_j' - (e\sin f)x_j, \tag{6c}$$
$$y_j'' = (1 + e\cos f)x_j'' - 2(e\sin f)x_j' - (e\cos f)x_j,$$

$$y(f) = \left[y_1(f)\;\; y_2(f)\;\; y_3(f)\;\; y_1'(f)\;\; y_2'(f)\;\; y_3'(f)\right]^T, \tag{6d}$$

$$\vec{a}(f) = \left[a_1(f)\;\; a_2(f)\;\; a_3(f)\right]^T, \tag{6e}$$

$$a_j(f) = \frac{\kappa^3 h^6}{\mu^4}\frac{T_j(f)}{m} \quad (j = 1, 2, 3), \qquad \kappa = \frac{1}{1 + e\cos f}. \tag{6f}$$

The parameter κ is determined from the well known equation of a Keplerian orbit (or equation of a conic section) where $\mu = GM_E$; h is the angular momentum; f is the true anomaly angle; x_1 is positive against the motion of the spacecraft, x_2 is positive along the radial direction, and x_3 is positive when the right handed system is completed. Equation (6c) is the mathematical transformation used to change from the x_j system to the y_j system. The x_j system contains the actual separation distance between the maneuvering and the reference (or target) spacecraft, and the y_j system has the same specified directions as the x_j system. The maneuvering spacecraft is assumed to have an applied thrust vector along the reference coordinate system, and the reference (or target) spacecraft is initially assumed to be acted on by a Newtonian gravitational force directed toward the center of the Earth.

It is known that the mass inside of the satellite will be changing with respect to the use of thrust for the correction of the drifts between any pair of satellites. The exhaust velocity [Carter and Humi 1987] is written as

$$m' = -\frac{h^3}{\mu^2}\frac{T(f)}{(1 + e\cos f)^2 C_s}, \tag{7}$$

where m is the mass of the satellite, T is the applied thrust for the maneuvering spacecraft and C_s is the effective exhaust velocity. Concerning the present problem, the difference between the initial and final true anomaly angle is assumed to be small enough such that the mass expended is much less in comparison to the initial mass (m_0) of the satellite during the correction of the drifts; hence, the actual mass ($m(f)$) of the satellite can be approximated by its initial mass ($m(f) \approx m_0$). Equation (6f) can be

reduced to

$$a_j = \frac{h^6}{\mu^4}\frac{T_m}{(1+e\cos f)^3 m_0}u_j(f) = bu_j(f)\kappa^3, \tag{8}$$

where T_m is the maximum thrust, and,

$$b = \frac{h^6}{\mu^4}\frac{T_m}{m_0}, \qquad u_j(f) = \frac{T_j(f)}{T_m} \quad (j = 1, 2, 3).$$

Equation (8) will be used to define the transformed thrust accelerations in (6a). If the mass of the satellite changes rapidly with respect to the correction of the drifts, (8) is not valid, and a minimization problem for a varying mass must be solved. Equation (8) will be implemented with the DLQR to determine the thrust consumption for the correction of the separation distance and the velocity drifts between any pair of satellites within the constellation.

Substituting (8) into (6a), the discrete form [Capó-Lugo and Bainum 2006a] of the linearized TH equations is expressed as

$$y(k+1) = \hat{A}(k)y(k) + \hat{B}(k)u(k), \tag{9a}$$

where $\hat{A}(f) = I + \Delta f\, A(f)$ and $\hat{B} = \Delta f\, B(f)$ are given by

$$\hat{A}(f) = \begin{bmatrix} 1 & 0 & 0 & \Delta f & 0 & 0 \\ 0 & 1 & 0 & 0 & \Delta f & 0 \\ 0 & 0 & 1 & 0 & 0 & \Delta f \\ 0 & 0 & 0 & 1 & 2\Delta f & 0 \\ 0 & 3\Delta f\kappa & 0 & -2\Delta f & 1 & 0 \\ 0 & 0 & -\Delta f & 0 & 0 & 1 \end{bmatrix}, \qquad \hat{B} = \begin{bmatrix} 0 & 0 & 0 \\ 0 & 0 & 0 \\ 0 & 0 & 0 \\ \Delta f\kappa^3 & 0 & 0 \\ 0 & \Delta f\kappa^3 & 0 \\ 0 & 0 & \Delta f\kappa^3 \end{bmatrix}, \tag{9b}$$

and further

$$\kappa(k) = \frac{1}{1+e\cos(f_L + k\Delta f)}, \tag{9c}$$

$$y(k) = \begin{bmatrix} y_1(k) & y_2(k) & y_3(k) & y_1'(k) & y_2'(k) & y_3'(k) \end{bmatrix}^T, \qquad f(k) = f_L + k\Delta f. \tag{9d}$$

Here I is the 6×6 identity matrix, f_L is the initial true anomaly angle, Δf is the sampling in the true anomaly angle, and k is an integer value representing the sample which is obtained at every sampling interval in the true anomaly angle. The integer k ranges from 0 to $N_f - 1$ where N_f is the last sample obtained in the solution of the linearized TH equations defined at the final true anomaly angle and is expressed as

$$N_f - 1 = \frac{f_F - f_L}{\Delta f},$$

where f_F and f_L, respectively, is the final and initial true anomaly angle in which the LQR will be used to correct the drifts between a pair of satellites within the constellation.

5. Station-keeping procedure (Stage 2)

In [Capó-Lugo and Bainum 2007], the LQR approach based on the Carter–Humi (CH) control scheme can be applied to every phase (size) of the tetrahedron constellation. In [Capó-Lugo and Bainum 2006a],

the discrete cost function for the CH was defined and written as

$$J(k) = \frac{\Delta f}{2} \sum_{k=0}^{N_f - 1} (y(k) - y_D)^T \tilde{Q}(k)(y(k) - y_D) + (u(k))^T \tilde{R}(k)(u(k)), \tag{10}$$

where $\tilde{Q}(k) = Q\kappa(k)$, $\tilde{R}(k) = R\kappa^2(k)$, and $y(k)$, y_D are the state vector and the desired state vector of the transformed system, respectively. The state and the desired state vector have dimensions of $n \times 1$.

In this case, the system of discrete linear equations can be defined similarly from (9a) as follows:

$$y(k+1) = \hat{A}(k)y(k) + \hat{B}(k)u(k) + \psi(k). \tag{11}$$

The system of linear equations in (9a) is expanded to include a perturbation vector, $\psi(k)$, to take into account outside forces due to the Earth, Moon, and/or Sun. The disturbance column vector in (11) is used to define the J2 perturbation that explains the oblateness of the Earth and is expressed as in [Battin 1999] by

$$\psi(k) = \begin{bmatrix} 0 \\ 0 \\ 0 \\ -\frac{3}{2} J_2 \frac{\mu}{r^2} \left(\frac{R_e}{r}\right)^2 (1 - 3\sin^2 i \sin^2(f_L + k\Delta f)) \\ -3J_2 \frac{\mu}{r^2} \left(\frac{R_e}{r}\right)^2 (\sin^2 i \sin(f_L + k\Delta f)\cos(f_L + k\Delta f)) \\ -3J_2 \frac{\mu}{r^2} \left(\frac{R_e}{r}\right)^2 (\sin i \cos i \sin(f_L + k\Delta f)) \end{bmatrix}, \tag{12}$$

where J_2 is approximated [Wertz and Larson 1999] to 1.08263×10^{-3}, R_e is the equatorial radius of the Earth, and i is the inclination angle. Equation (12) will not require a transformation with (6c) because $\psi(k)$ is defined in terms of the mean orbital elements of the satellites in the proposed constellation [Carpenter et al. 2003], as shown in Table 2.

In [Capó-Lugo and Bainum 2006a], the solution of the DLQR problem is obtained but is rewritten here for the y_j system as

$$K(k) = \Delta f \tilde{Q}(k) + \hat{A}^T(k)K(k+1)[I + S(k)K(k+1)]^{-1}\hat{A}(k), \tag{13a}$$

$$g(k) = -\Delta f \tilde{Q}(k)y_D - \hat{A}^T(k)K(k+1)[I + S(k)K(k+1)]^{-1}[S(k)g(k+1) - \psi(k)] + \hat{A}^T(k)g(k+1), \tag{13b}$$

$$y(k+1) = [I + S(k)K(k+1)]^{-1}[\hat{A}(k)y(k) - S(k)g(k+1) + \psi(k)], \tag{13c}$$

$$u(k) = -[\Delta f \tilde{R}(k)]^{-1}\hat{B}^T(k)[K(k+1)y(k+1) + g(k+1)], \tag{13d}$$

where

$$S(k) = \hat{B}(k)[\Delta f \tilde{R}(k)]^{-1}\hat{B}^T(k). \tag{13e}$$

Equations (13a) and (13b) are the digital forms of the Riccati and adjoint Riccati equations. The solution of the DLQR follows the same procedure as explained in [Capó-Lugo and Bainum 2006a]. With this procedure, the satellites will be reconfigured to the proposed tetrahedron constellation at the following apogee point.

6. Results

The complete deployment and station-keeping procedure are defined in the following steps: (1) two ΔV procedures are used to transfer the satellites from a circular orbit to their respective elliptical orbits; (2) then, the DLQR control scheme is used to correct the drifts in the separation distances and velocities between any pair of satellites such that the proposed tetrahedron constellation is obtained at the following apogee point.

Stage 1. The software package used in the simulation for the transfer from a circular to the elliptical orbit is a released version 6.2 of the Satellite Tool Kit software package (STK) [STK 2003]. The company has kindly provided an educational license to use many of the STK capabilities. The STK software is very user friendly and allows simulation in real time. The STK package offers different options for different sets of data input: one for the basic properties, one for the graphic visualization in two dimensions and three dimensions, and other modules for the constraints imposed on the problem.

The STK has different orbit propagators to simulate the NASA Benchmark Tetrahedron Constellation. These orbit propagators are the two body, J2 perturbation, High Precision Orbit Propagator (HPOP), and the Astrogator. In [Capó-Lugo and Bainum 2005; 2006b], the STK was used with the two body, J2 perturbation, and the HPOP orbit propagators to simulate the tetrahedron constellation for a period of time. The Astrogator orbit propagator is used here to input the impulse maneuvers detailed in Steps 1-5 in Section 3 to determine if the satellites reach the final elliptical orbit at the same time. This orbit propagator provides different instructions to define the ΔV maneuvers at the perigee and apogee point for every satellite; in addition, the Astrogator has an instruction that defines the transfer point of the four satellites. Using this instruction in the orbit propagator, the transfer point is defined when the true anomaly angle is equal to 90°; in this way, the desired argument of perigee for the elliptical orbit can be obtained for every satellite.

In Section 3, the four satellites are located in a circular orbit in which its radius is equal to the radius of perigee for phase I, and the inclination angle is equal to 18.5°. The initial time [Carpenter et al. 2003] for the simulation is June 21, 2009 at 00:00:00 UTCG. This initial date and time was defined in the NASA Benchmark Tetrahedron Constellation problem [Carpenter et al. 2003]. The simulation is performed without perturbations because the satellites will not be in the initial circular orbit for a long period of time such that the perturbations due to the Earth can build up through time. Figure 4 shows the initial

Figure 4. Initial satellite locations in the circular orbit.

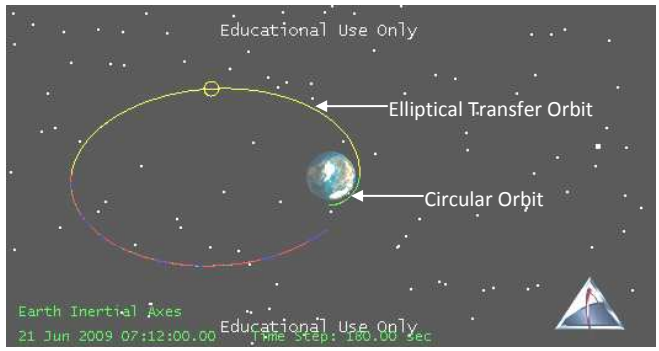

Figure 5. Satellites in the transfer elliptical orbit.

location of the four satellites in the circular orbit. The locations of the satellites are shown with a circle, but the four satellites are not shown because of the vantage point of view used in the STK software. The four satellites have the same separation distance as shown in Figure 2 and mentioned in Section 3. The difference in the true anomaly angle (δf) is assumed to be equal to 0.5°.

When every satellite reaches a true anomaly angle equal to 90°, the first burn at the transfer point is performed such that the satellites are maneuvered into the elliptical transfer orbit. As said earlier, the Astrogator is instructed to perform a ΔV maneuver for every satellite when the true anomaly angle is 90°. Figure 5 shows the satellites in the elliptical transfer orbit. Once more, the position of the satellites is shown with a circle in the elliptical transfer orbit, and, through the simulation, the satellites travel near each other such that the four satellites will arrive at the apogee point at the same time. The STK provides different tables to show various data points like the position, velocity, orbital elements, etc. for any satellite used in the simulation. The data defining the separation distance between any pair of satellites is used to determine if the satellites violate the separation distance constraints of the NASA Benchmark Tetrahedron Constellation [Carpenter et al. 2003]. This constraint says that the satellites can not have a separation distance less than 1 km at any other point in the orbit, excluding the apogee point. At the apogee point, the nominal separation distance condition is 10 ± 1 km between any pair of satellites within the constellation. With these data tables, it is found that the minimum separation distance in the transfer elliptical orbit between any pair of satellites is greater than 13 km for a difference in the true anomaly angle of 0.5°. This shows that no pair of satellites violates the separation distance constraints in the elliptical transfer orbit.

Figure 6 shows the simulation after the satellites reach the apogee point in the elliptical transfer orbit when the Astrogator is performing the last ΔV maneuver explained in step 5 (page 842). In Figure 6, the satellites arrive at the apogee point at the same time, but there are drifts in the separation distance between any pair of satellites within the constellation: the separation distances range from 10 to 28 kilometers (for $\delta f = 0.5°$). For this reason, the constellation will be corrected with the DLQR to obtain the proposed tetrahedron constellation at the following apogee point; in addition, SH must be located in its out-of-plane position to obtain the final formation.

The difference in the true anomaly angle (δf) can be analyzed with the STK to determine how δf affects the separation distances between any pair of the satellites at the final apogee point. The difference in the true anomaly angle used in the previous simulations is 0.5°, but this δf will be increased to 1 degree and decreased to 0.3° to determine the effects on the separation distance at the final apogee point.

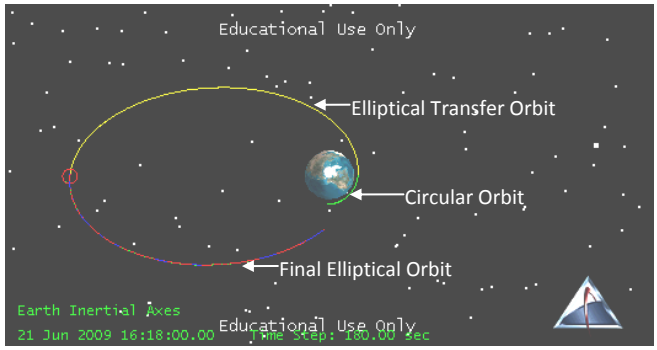

Figure 6. Satellites at the apogee point of the final elliptical orbit.

δf	SA-SB	SA-SC	SA-SH	SB-SC	SB-SH	SC-SH
0.3°	15.276	10.696	5.406	14.459	13.875	5.290
0.5°	14.080	17.960	9.008	20.689	15.258	8.952
1°	15.196	35.958	18.018	44.465	27.970	17.940

Table 5. Separation distances (in km) between pairs of satellites for various δf.

Table 5 shows the separation distance between any pair of satellites within the constellation for the chosen values of δf. In Table 5, δf must be constrained between 0 and 1 degree such that a minimum separation distance can be obtained at the apogee point. For the pair SA-SB, the separation distance does not significantly diminish with a decrease in the δf, but, for the other pairs of satellites, the separation distance is decreased as δf decreases. When $\delta f = 0.3$, the separation distance between any pair of satellites is near the 10 km range; in this way, the DLQR can be efficiently used to correct the drifts between any pair of satellites to obtain the desired configuration at the final apogee point.

Table 6 shows the orbital elements and the position of the four satellites at the final apogee point. It can be seen from Table 6 that the four satellites arrive at the apogee point at the same time. Comparing Table 2 with Table 6, SB can be used as the reference satellite because it has similar orbital elements as in Table 2. For this reason, SB will be used as the target spacecraft to correct the other three satellites such that, at the following apogee point, the proposed tetrahedron constellation can be obtained.

	SA	SB	SC	SH
a (km)	42,091.02	42,095.44	42,093.47	42,091.02
e	0.818162	0.818359	0.818270	0.818124
i (degrees)	18.5	18.5	18.5	18.5
Ω (degrees)	0	0	0	0
ω (degrees)	90	90	90	90
f (degrees)	180.056	180.055	180.043	180.059

Table 6. Initial orbital elements for the four satellites within the constellation (Phase I).

	SA	SB	SC	SH
X (km)	410.539171	404.465887	399.847473	405.135249
Y (km)	−72567.835478	−72581.128031	−72568.133913	−72567.985691
Z (km)	−24280.858097	−24285.305723	−24280.957952	−24280.908358
V_X (km/sec)	0.973120	0.972665	0.973407	0.973122
V_Y (km/sec)	0.027229	0.026829	0.026512	0.026871
V_Z (km/sec)	0.009111	0.008977	0.008871	0.008991

Table 7. Initial coordinates and velocities for the four satellites at the apogee point after the transfer maneuver.

Stage 2. The initial positions and velocities at the apogee point for the four satellites are obtained from the STK data tables to determine the initial conditions for the DLQR active control scheme. Table 7 shows the initial coordinates and velocities of the four satellites at the final apogee point after the final transfer maneuver. The values shown in Table 7 are obtained for a difference in the true anomaly angle of 0.3° and are used to calculate the difference between the reference and the maneuvering satellites because the separation distances are near the 10 km in comparison with the other values for the difference in the true anomaly angle shown in Table 5.

It is known that the reference satellite is SB, and the maneuvering satellites are SA, SC, and SH. The difference between the reference satellite and the maneuvering satellites for the nominal coordinates are known as the nominal separation distance. This difference is obtained from Table 1 that defines the desired coordinates and velocities for the four satellites. The same calculation is performed for the initial coordinates and velocities shown in Table 7. This difference between the initial coordinates and velocities is known as the initial separation distance.

In the DLQR control scheme [Capó-Lugo and Bainum 2006a], the initial conditions are defined from the difference between the satellite initial and nominal coordinates and velocities for these three pairs of satellites. These initial conditions are the drifts that must be corrected such that, at the following apogee point, the NASA Benchmark Tetrahedron Constellation can be obtained with the required separation distance conditions [Carpenter et al. 2003]. Table 8 shows the drifts for the separation distance and velocities for these pairs of satellites.

	SB-SA	SB-SC	SB-SH
$x_1(f_L) = X_S - X_N$ (km)	−14.7335	4.6184	−3.5561
$x_2(f_L) = Y_S - Y_N$ (km)	−8.5510	−2.7640	−10.2446
$x_3(f_L) = Z_S - Z_N$ (km)	−2.8611	−1.1748	4.9325
$x_1'(f_L) = X_S' - X_N'$ (m/sec)	−0.3190	−0.4274	−0.1073
$x_2'(f_L) = Y_S' - Y_N'$ (m/sec)	−0.4000	0.3170	−0.0420
$x_3'(f_L) = Z_S' - Z_N'$ (m/sec)	−0.1340	0.1060	−0.0140

Table 8. Initial conditions for the digital LQR control scheme.

The simulations with the DLQR will begin at the apogee point in which the four satellites arrive after the second ΔV maneuver (Figure 6) and will finish at the following apogee point. At this final apogee point, the separation distance and velocities for the four satellites will be satisfied. In reference [Capó-Lugo and Bainum 2006a], it is demonstrated that the DLQR is better approximated when the sampling in the true anomaly angle is 0.1 radians. The Q and R matrices are 6×6 positive definite and 3×3 positive semidefinite diagonal matrices, respectively. The R matrix is chosen to maintain a minimum consumption of fuel, and the Q matrix is obtained from different simulations to determine a minimum time problem as shown in reference [Capó-Lugo and Bainum 2007]. In this simulation, the weights for the Q and R matrices are diag[20 20 20 1 1 1] and diag[1 1 1], respectively. As explained in reference [Capó-Lugo and Bainum 2006a], the positions are weighted more than the velocities because the DLQR will compensate more the positions that are multiplied by the varying coefficient term, κ.

The thrust system assumed for this simulation is the ion thruster. The ion thruster has a maximum thrust range between 5×10^{-5} and 0.5 N [Wertz and Larson 1999]. In these simulations, it is assumed that the maximum thrust is equal to 0.5 N. After the final Hohmann transfer maneuvers, the satellites will be in the elliptical orbit defined by the orbital elements of phase I (Table 6). For all the simulations, y_D is set to zero.

Figure 7 shows the correction of the drifts in the separation distance and velocity for the X direction for the three pairs of satellites. It can be seen that SB-SC requires less amount of thrust than SB-SH and SB-SA. For the three cases, the maximum value of the optimal control is 10^{-3} N in which the DLQR provides a very good response and optimal use of the thrust in the satellite. The assumption taken between the initial and final mass in the satellite is approximately correct because of this small expenditure of thrust. In addition, the maximum thrust for the ion propulsion can be reduced, or the R matrix can be changed to a different weight forcing the maximum value of the thrust level in Figure 7 to decrease. For this case, the correction of the drifts and the optimal control came to rest in less than half of an orbit.

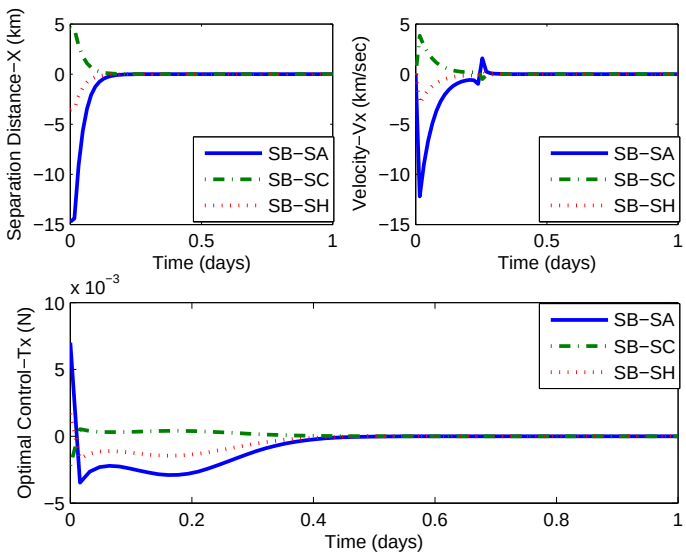

Figure 7. Correction of the separation distance and velocity for the satellites in the X direction.

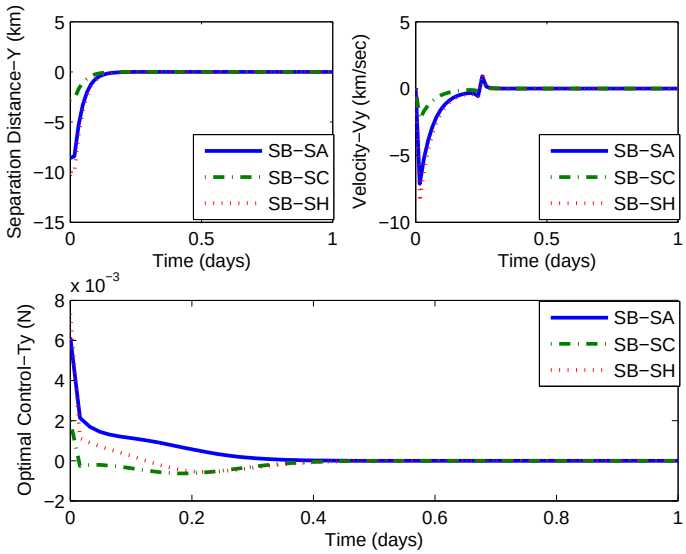

Figure 8. Correction of the separation distance and velocity for the satellites in the Y direction.

Figure 8 shows the correction for the separation distance and velocity for the three pairs of satellites in the Y direction. In this case, SB-SH requires a higher amount of thrust in comparison to SB-SC and SB-SA because SH is moving to its out-of-plane position to form the tetrahedron constellation. The correction of the separation distance for the three cases happens near the apogee point because of the weight chosen for the Q matrix. With this weight, the positions, which are multiplied by the varying term (κ), are corrected faster than the velocities because, in the TH equations, the coefficients in the velocity terms are multiplied by constants. The maximum value for the optimal control is 10^{-3} N, and the optimal control comes into rest in less than 0.5 days; in other words, the controller comes to rest before the satellites reaches the first perigee point after the correction begins.

Figure 9 shows the correction for the separation distance and the velocity for the satellites along the Z direction. In this case, SB-SH also requires a higher consumption of thrust than SB-SC and SB-SA because, as said earlier, SH will move into a different orbital plane to form the proposed tetrahedron constellation [Carpenter et al. 2003]. It is also seen that the corrections of the separation distance, the velocity, and the optimal control take less than half of an orbit. In addition, the maximum value of the optimal control is approximately 10^{-3} N and comes to rest in less than half of an orbit.

In all the simulations, the correction for the separation distances and the velocities will be performed before the satellites reach the first perigee point after the correction begins. In addition, the optimal control shows a small consumption of fuel for the three pairs of satellites. The assumption made about the mass inside of the satellite can be used in the DLQR active control scheme for the correction of the separation distance and velocity drifts. Hence, the NASA Benchmark Tetrahedron Constellation will be reconfigured at the following apogee point, and, in [Capó-Lugo and Bainum 2007], it was shown that the satellites will maintain the separation distance constraints for a limited number of complete orbits when the perturbations due to the Earth are acting on the satellites.

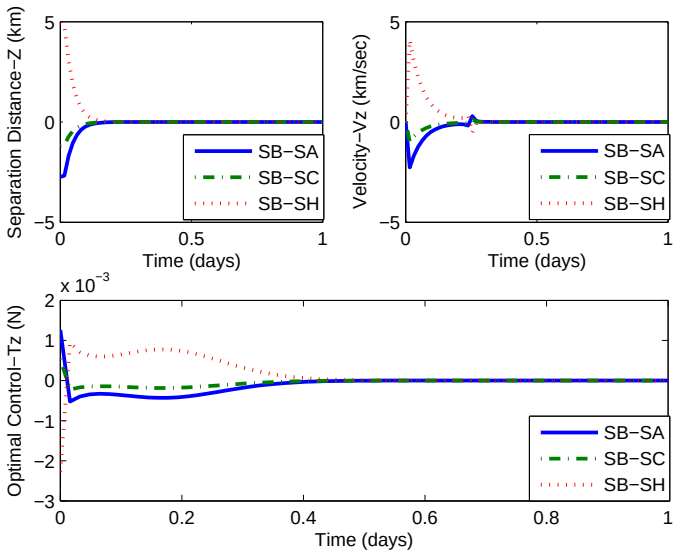

Figure 9. Correction of the separation distance and velocity for the satellites in the Z direction.

7. Remarks

A different solution for the deployment of the NASA Benchmark Tetrahedron Constellation is provided. The mathematical procedures are much simpler than in [Williams and Trivailo 2006; Huntington et al. 2006; Huntington and Rao 2006] that use the Pseudospectral methods. All the techniques used to obtain the proposed tetrahedron constellation [Carpenter et al. 2003] are known and can be easily implemented for this problem.

In the deployment from the circular orbit to the elliptical orbit, the difference in the true anomaly angle between the satellites in the circular orbit must be less than 0.5° to obtain a minimum value in the separation distance between any pair of satellites at the final apogee point of the transfer maneuver. After the final Hohmann maneuver is performed, the satellites will reach the apogee point at the same time.

After the transfer maneuver is finished, the digital linear quadratic regulator is used to finally correct the drifts between the three pairs of satellites. It is shown that the satellites have a very small consumption of energy in which the mass inside of the satellites will not be changing rapidly. The satellite in the out-of-plane motion will require a higher thrust consumption to obtain the final tetrahedron constellation.

In conclusion, this work contributes, for the first time, a different solution for the deployment and station-keeping of the NASA Benchmark Tetrahedron Constellation when Hohmann transfer maneuvers and a digital linear quadratic regulator are combined to obtain the desired formation. Using both techniques, a small consumption of fuel is obtained for the deployment procedure of the proposed tetrahedron constellation.

References

[Bainum et al. 2005] P. M. Bainum, A. Strong, Z. Tan, and P. A. Capó-Lugo, "Techniques for deploying elliptically orbiting constellations in along-track formation", *Acta Astronaut.* **57**:9 (2005), 685–697.

[Battin 1999] R. H. Battin, *An introduction to the mathematics and methods of astrodynamics*, Rev. ed., Chapter 10, pp. 471–514, AIAA, Reston, VA, 1999.

[Capó-Lugo and Bainum 2005] P. A. Capó-Lugo and P. M. Bainum, "Strategy for satisfying distance constraints for the NASA benchmark tetrahedron constellation", pp. 775–793 in *Space flight mechanics 2005: proceedings of the AAS/AIAA Space Flight Mechanics Conference* (Copper Mountain, CO, 2005), vol. 1, edited by D. A. Vallado et al., Advances in the Astronautical Sciences **120**, American Astronautical Society, San Diego, CA, 2005. Paper #AAS 05-153.

[Capó-Lugo and Bainum 2006a] P. A. Capó-Lugo and P. M. Bainum, "Digital LQR control scheme to maintain the separation distance of the NASA benchmark tetrahedron constellation", in *AIAA/AAS Astrodynamics Specialist Conference and Exhibit* (Keystone, CO, 2006), AIAA, Reston, VA, 2006. Paper #AIAA 2006-6014. Reprinted in *Acta Astronaut.* **65**:7–8 (2009), 1058–1067, DOI 10.1016/j.actaastro.2009.03.040.

[Capó-Lugo and Bainum 2006b] P. A. Capó-Lugo and P. M. Bainum, "Implementation of the strategy for satisfying distance constraints for the NASA benchmark tetrahedron constellation", pp. 1463–1482 in *Astrodynamics 2005: proceedings of the AAS/AIAA Astrodynamics Specialists Conference* (Lake Tahoe, CA, 2005), vol. 2, edited by B. G. Williams et al., Advances in the Astronautical Sciences **123**, American Astronautical Society, San Diego, CA, 2006. Paper #AAS 05-344.

[Capó-Lugo and Bainum 2007] P. A. Capó-Lugo and P. M. Bainum, "Active control schemes to satisfy separation distance constraints", *J. Guid. Control Dyn.* **30**:4 (2007), 1152–1156.

[Carpenter et al. 2003] R. J. Carpenter, J. A. Leitner, D. C. Folta, and R. D. Burns, "Benchmark problems for spacecraft formation flying missions", in *AIAA Guidance, Navigation, and Control Conference and Exhibit* (Austin, TX, 2003), AIAA, Reston, VA, 2003. Paper #AIAA 2003-5364.

[Carter and Humi 1987] T. Carter and M. Humi, "Fuel-optimal rendezvous near a point in general Keplerian orbit", *J. Guid. Control Dyn.* **10**:6 (1987), 567–573.

[Dow et al. 2004] J. Dow, S. Matussi, M. Dow, Roberta, M. Schmidt, and M. Warhaut, "The implementation of the cluster II constellation", *Acta Astronaut.* **54**:9 (2004), 657–669.

[Huntington and Rao 2006] G. T. Huntington and A. V. Rao, "Optimal reconfiguration of a tetrahedral formation via a Gauss pseudospectral method", pp. 1337–1358 in *Astrodynamics 2005: proceedings of the AAS/AIAA Astrodynamics Specialists Conference* (Lake Tahoe, CA, 2005), vol. 2, edited by B. G. Williams et al., Advances in the Astronautical Sciences **123**, American Astronautical Society, San Diego, CA, 2006. Paper #AAS 05-338.

[Huntington et al. 2006] G. T. Huntington, D. A. Benson, and A. V. Rao, "Post-optimality evaluation and analysis of a formation flying problem via a Gauss pseudospectral method", pp. 1359–1377 in *Astrodynamics 2005: proceedings of the AAS/AIAA Astrodynamics Specialists Conference* (Lake Tahoe, CA, 2005), vol. 2, edited by B. G. Williams et al., Advances in the Astronautical Sciences **123**, American Astronautical Society, San Diego, CA, 2006. Paper #AAS 05-339.

[Lawden 1963] D. F. Lawden, *Optimal trajectories for space navigation*, Butterworths, London, 1963.

[STK 2003] *Satellite tool kit software*, Version 5.0, Analytical Graphics, Malvern, PA, 2003.

[Wertz and Larson 1999] J. R. Wertz and W. J. Larson (editors), *Space mission analysis and design*, 3rd ed., Space Technology Library **8**, Microcosm, El Segundo, CA, 1999.

[Williams and Trivailo 2006] P. Williams and P. Trivailo, "Numerical approach designing and deploying satellite formations", in *Proceedings of the 25th International Symposium on Space Technology and Science* (Kanazawa, 2006), Japan Society for Aeronautical and Space Sciences, Tokyo, 2006. Paper #2006-d-40.

Received 11 Mar 2008. Revised 13 May 2009. Accepted 17 May 2009.

PEDRO A. CAPÓ-LUGO: pcapo@howard.edu
Department of Mechanical Engineering, Howard University, 2300 Sixth Street, NW, Washington, DC 20059, United States
Current address: EV41, Guidance, Navigation and Control Systems Design and Analysis Branch, NASA Marshall Space Flight Center, Huntsville, AL 35812, United States

PETER M. BAINUM: pbainum@fac.howard.edu
Department of Mechanical Engineering, Howard University, 2300 Sixth Street, NW, Washington, DC 20059, United States